Inorganic Chemistry

Open Access
This article is licensed under CC-BY-NC-ND 4.0

pubs.acs.org/IC
Communication

Sn/As-Based P_4-Analogous Zintl Anions $(Sn_2As_2)^{2-}$ and $(HSn_3As)^{2-}$

Maximilian Kubis, Benjamin Peerless, Yannick J. Franzke,* and Stefanie Dehnen*

Cite This: https://doi.org/10.1021/acs.inorgchem.6c04492
Read Online

ACCESS | Metrics & More | Article Recommendations | Supporting Information

ABSTRACT: Despite being composed of atoms of notably different atomic radii, the P_4-analogous anion $(Sn_2As_2)^{2-}$ was obtained upon treatment of a ternary solid with the nominal composition 'K_2SnAs' with ethane-1,2-diamine and *crypt*-222 by careful control of the reaction conditions and workup. X-ray diffraction and ^{119}Sn NMR studies aided by sophisticated theoretical predictions showed that this anion co-crystallizes together with the protonated species $(HSn_3As)^{2-}$. The co-crystallization requires protonation of the latter to match the 2− charge of the other dianion in the salt. The studies also show that the P_4-analogous anions are readily oxidized to give $(Sn_7As_2)^{2-}$. *In situ* investigations using NMR revealed the co-existence of $(Sn_2As_2)^{2-}$ and $(HSn_3As)^{2-}$ in solution. The study showcases the first binary P_4-analogous Zintl anions comprising the elemental combination of Sn and As, which will be studied in terms of their reactivity toward d-block and f-block metal compounds in future work.

The treatment of Zintl phases with highly polar solvents, typically ethane-1,2-diamine (*en*) or ammonia, in the presence of sequestering agents like 4,7,13,16,21,24-hexaoxa-1,10-diazabicyclo[8.8.8]hexacosane (*crypt*-222) or 1,4,7,10,13,16-hexaoxacyclooctadecane (18-*crown*-6), is the most commonly used method of obtaining salts of homoatomic or heteroatomic anions of p-block (semi)metals.[1−4]

A particularly interesting family of p-block anions that have grown in prominence recently are binary dianions of the type $(TrPn_3)^{2-}$ or $(Tt_2Pn_2)^{2-}$ (Tr/Tt/Pn = group 13/14/15 element). Isoelectronic to the archetypal P_4 tetrahedron, these compounds have been shown to be versatile starting materials for the formation of larger clusters upon reactions with d- and f-block metal compounds.[2−9] Yet, to date, of all 32 possible combinations of $(TrPn_3)^{2-}$ or $(Tt_2Pn_2)^{2-}$, only 12 have been synthetically accessed[7,10−18] and several have been suggested to be inherently inaccessible.[18,19] A nuanced interplay between the relative size and electron affinities of the atoms involved has been made responsible for that. For example, $(Sn_2Sb_2)^{2-}$ and $(Sn_2Bi_2)^{2-}$ can be prepared as their $[K(crypt\text{-}222)]^+$ salts in multigram scale. $(InSb_3)^{2-}$ and $(TlSb_3)^{2-}$ are metastable in solution toward formation of larger anions,[18] and $(GaBi_3)^{2-}$ and $(Ge_2Bi_2)^{2-}$ could not be crystallized, while salts of $(Ga_2Bi_{16})^{4-}$ and $(Ge_4Bi_{14})^{4-}$ have been obtained instead.[20,21]

For the lighter elements, atom-exchanged variants have been observed in ternary clusters containing $(Ge_3P)^{3-}$ or $(Ge_3As)^{3-}$ moieties,[9,16] and treatment of a ternary solid 'KGeP' with *en* was recently shown to yield protonated $(HGe_3P)^{2-}$ only, instead of $(Ge_2P_2)^{2-}$.[22]

One combination yet to be investigated is the Sn/As system, to enable future studies of the reactivity of a species situated between lighter and heavier (semi)metals toward d- and f-block metal complexes. When considering the postulated conditions required for a stable P_4-analogous p-block anion, $(Sn_2As_2)^{2-}$ pushes the limits on the balance of both atomic radii and electron affinities and was therefore suspected to be potentially inaccessible.[19] To date, there are only two examples of (larger) anions containing both arsenic and tin: $(SnAs_{15})^{3-}$ [23] and $[As_3NbSn_3As_3]^{3-}$.[24] The former is obtained by the reaction between SnI_2 and K_3As_7 in *en* and the latter by treatment of the quaternary Zintl phase $K_8NbSnAs_5$ with *en*. We endeavored to investigate the behavior of 'K_2SnAs' under such conditions, as 'K_2SnPn' is commonly used for synthesizing the heavier pnictogen congeners.[4]

Herein, we describe the observations made upon treatment of 'K_2SnAs' with en, yielding the $(Sn_2As_2)^{2-}$ anion and the protonated analogue $(HSn_3As)^{2-}$. Additionally, $(Sn_7As_2)^{2-}$ was obtained indicating the metastability of these anions. We combined sophisticated quantum chemical calculations with in-depth NMR spectroscopic and mass spectrometric studies to provide a deeper understanding of the processes in solution.

To prepare 'K_2SnAs', the elements were sealed in a Nb tube inside a silica glass tube, which was then sealed under vacuum, in the appropriate stoichiometry. After heating and tempering inside a chamber oven (see Supporting Information, Section 1), a metallic powder was obtained, which by powder X-ray diffraction (PXRD, Figure S5) was found to contain a new quaternary phase, $K_{13}Nb_2Sn_2As_9$ (**1**), and at least one other phase of poor crystallinity. Single crystal X-ray diffraction (SC-XRD) showed the $[Nb_2Sn_2As_9]^{13-}$ anion (Figure 1) to be a condensed form of the previously described $[NbSnAs_5]^{8-}$ anion,[24] bridged through an As atom. More structural details are shown in Figures S1 and S2. The formation of the ternary anion in **1** is aligned with the tendency of As-based Zintl phases/reaction mixtures to corrode the Nb ampules and form

Received: August 22, 2026
Revised: October 3, 2026
Accepted: October 6, 2026

ACS Publications
© XXXX The Authors. Published by American Chemical Society

Downloaded from pubs.acs.org/inocaj/article-pdf/doi/10.1021/acs.inorgchem.6c04492/6918915/acs.inorgchem.6c04492.pdf by KIT BIBLIOTHEK user on 16 November 2026

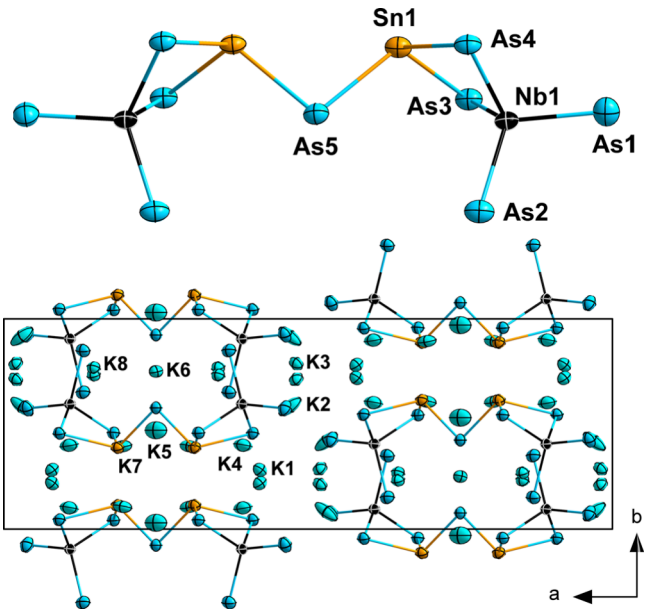
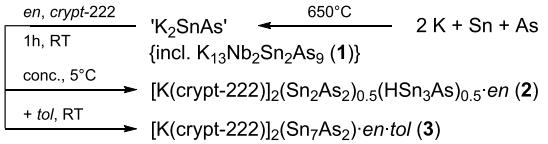


Figure 1. Molecular structure of the ternary $[Nb_2Sn_2As_9]^{13-}$ anion in **1** (top) and extended unit cell (bottom). Thermal ellipsoids drawn at 50% probability.

Nb-containing anions, such as $[Nb@As_8]^{3-}$ or $[Nb@Ge_8As_6]^{3-}$.[25,26]

Efforts to improve the crystallinity of the K/Sn/As material and identify other components were unsuccessful. Nevertheless, the treatment of this material with two equivalents of *crypt*-222 in *en* was attempted, which afforded a dark suspension after 1 h of stirring. Upon filtration, we obtained different crystalline products depending on the crystallization methods employed (Scheme 1).

Scheme 1. Formation of Compounds 1, 2, and 3, Illustrated by Non-stochiometric Reaction Schemes



Concentration of the solution and storage at 5 °C yields dark red crystals of $[K(crypt\text{-}222)]_2(Sn_2As_2)_{0.5}(HSn_3As)_{0.5}\cdot en$ (**2**). When the solution is simply layered with toluene and stored for several days at room temperature, orange crystals of $[K(crypt\text{-}222)]_2(Sn_7As_2)\cdot en\cdot tol$ (**3**) are obtained alongside an orange powder identifiable as $[K(crypt\text{-}222)]_2Sn_5$.[27] As compound **2** and $[K(crypt\text{-}222)]_2Sn_5$ are poorly differentiated by PXRD, we used NMR to confirm the presence of $[K(crypt\text{-}222)]_2Sn_5$ (see Figure 2c). The oxidative formation of Sn_5^{2-} and $(Sn_7As_2)^{2-}$ is postulated to occur due to the metastable nature of $(Sn_2As_2)^{2-}$ in solution, which apparently can be slowed down enough at 5 °C to allow for **2** to crystallize. Increasing the reaction time in *en* to 24 h, upon crystallization of **2**, the previously reported salt of a ternary cluster, $[K(crypt\text{-}222)]_3[As_3NbSn_3As_3]$,[24] is obtained as a second crystalline product, most likely arising from the presence of **1** in the starting intermetallic solid mixture.

$[K(crypt\text{-}222)]_2(Sn_2As_2)_{0.5}(HSn_3As)_{0.5}\cdot en$ (**2**) crystallizes in the monoclinic space group $P2_1$ with two formula units per unit cell. Assignment of the Sn and As atomic positions was made by free refinement of the site occupation factors (s.o.f.) upon an Sn:As 0.5:0.5 initial occupancy at each of the four corners of the polyhedron. It was found for three of the sites there was a greater preference for Sn, indicated by the corresponding s.o.f. in positions 1 (0.9), 2 (0.8), and 3 (0.6), as labeled in Figure 2a, and for As in position 4 (0.8). Both P_4-analogous anions share the same positions within the crystal structure, and therefore the presence of $(HSn_3As)^{2-}$ can only be inferred from the average bond lengths of the modeled anion, which in this case is 2.791 Å. The average bond length calculated with density functional theory (DFT) is distinctly shorter for $(Sn_2As_2)^{2-}$, 2.705 Å, while is noticeably longer for $(HSn_3As)^{2-}$, 2.851 Å (Figure S4). A clearly defined stoichiometry of both anionic components can only be estimated, and a 1:1 ratio fits very well with the calculated average.

Electrospray ionization mass spectrometry (ESI-MS) measurements of a fresh N,N-dimethylformamide (DMF) solution of single crystals of **2** (Figure S15) show signals corresponding to $(HSn_2As_2)^-$ at m/z = 388.6537 and $(SnAs)^-$ at m/z = 194.8242, serving as indirect mass spectrometric evidence for $(Sn_2As_2)^{2-}$. The ^{119}Sn NMR spectrum of **2** dissolved in DMF-d_7 (Figure 2a) further illustrates the presence of both anions. A single sharp resonance at −1672 ppm with $^1J(^{119}Sn, ^{117}Sn)$ = 1528 Hz is consistent with $(Sn_2As_2)^{2-}$, which is similar in shape and slightly shifted to higher field in comparison to the ^{119}Sn resonances of $(Sn_2Sb_2)^{2-}$ in DMF and $(Sn_2Bi_2)^{2-}$ in *en* (−1606 and −1575 ppm, respectively).[28,29] Two broader resonances at −1338 ppm and underneath the sharp resonance of $(Sn_2As_2)^{2-}$ were assigned to $(HSn_3As)^{2-}$, along with a resonance at −14.79 ppm in the ^{1}H NMR spectrum (Figure 2b). Two other weaker resonances appear in the ^{119}Sn NMR spectrum at −1001 pm, which could be assigned to $(Sn_7As_2)^{2-}$, and at −869 ppm, an impurity which could not be assigned. Furthermore, a ^{119}Sn NMR spectrum of the crystalline product obtained after 24 h treatment with *en* showed a resonance at −1376 ppm in addition to the resonances observed previously, which we assign to the $[As_3NbSn_3As_3]^{3-}$ anion (see Figure S11). Figure 2c shows the ^{119}Sn NMR spectrum in DMF-d_7 of $(Sn_7As_2)^{2-}$ for comparison (details to be found in the Supporting Information, Section 7).

^{119}Sn NMR resonances in Figure 2 were assigned with the aid of quantum chemical studies using relativistic spin−orbit all-electron exact two-component (SO-X2C) theory[30−35] at the TPSSh/x2c-TZVPall-s DFT level (x2c-SVPall bases for 25 DMF molecules that were considered explicitly).[36,37] Table 1 lists the calculated and experimental values for the DMF solution; more data are provided in Tables S5 and S6.

Ge/P- and Ge/As-based anions with a 3:1 combination of atoms have previously been reported, also within larger cluster products based on them, as well as the oxidative growth of the smaller units.[15,16] *In situ* ^{119}Sn NMR measurements were recorded on the solution in *en*, showing four resonances at −1239, −1317, −1674, and −1747 ppm (see Figure 2d). The resonances at −1239 and −1747 ppm can be assigned to Sn_9^{4-} [38] and $(Sn_2As_2)^{2-}$, respectively, as confirmed by a spectrum of **2** recorded in *en* (Figure S14). A tentative assignment of the major resonance at −1674 ppm could be made to $(Sn_3As)^{3-}$ on the basis of the theoretical prediction in DMF. Lastly, the resonance at −1317 ppm was assigned to Sn_5^{2-} (discussed below). No resonance is observed for $(HSn_3As)^{2-}$ in the ^{119}Sn NMR. Most likely, the low

Downloaded from pubs.acs.org/inocaj/article-pdf/doi/10.1021/acs.inorgchem.6c04492/6918961 5/acs.inorgchem.6c04492.pdf by KIT BIBLIOTHEK user on 16 November 2026

https://doi.org/10.1021/acs.inorgchem.6c04492
Inorg. Chem. XXXX, XXX, XXX−XXX

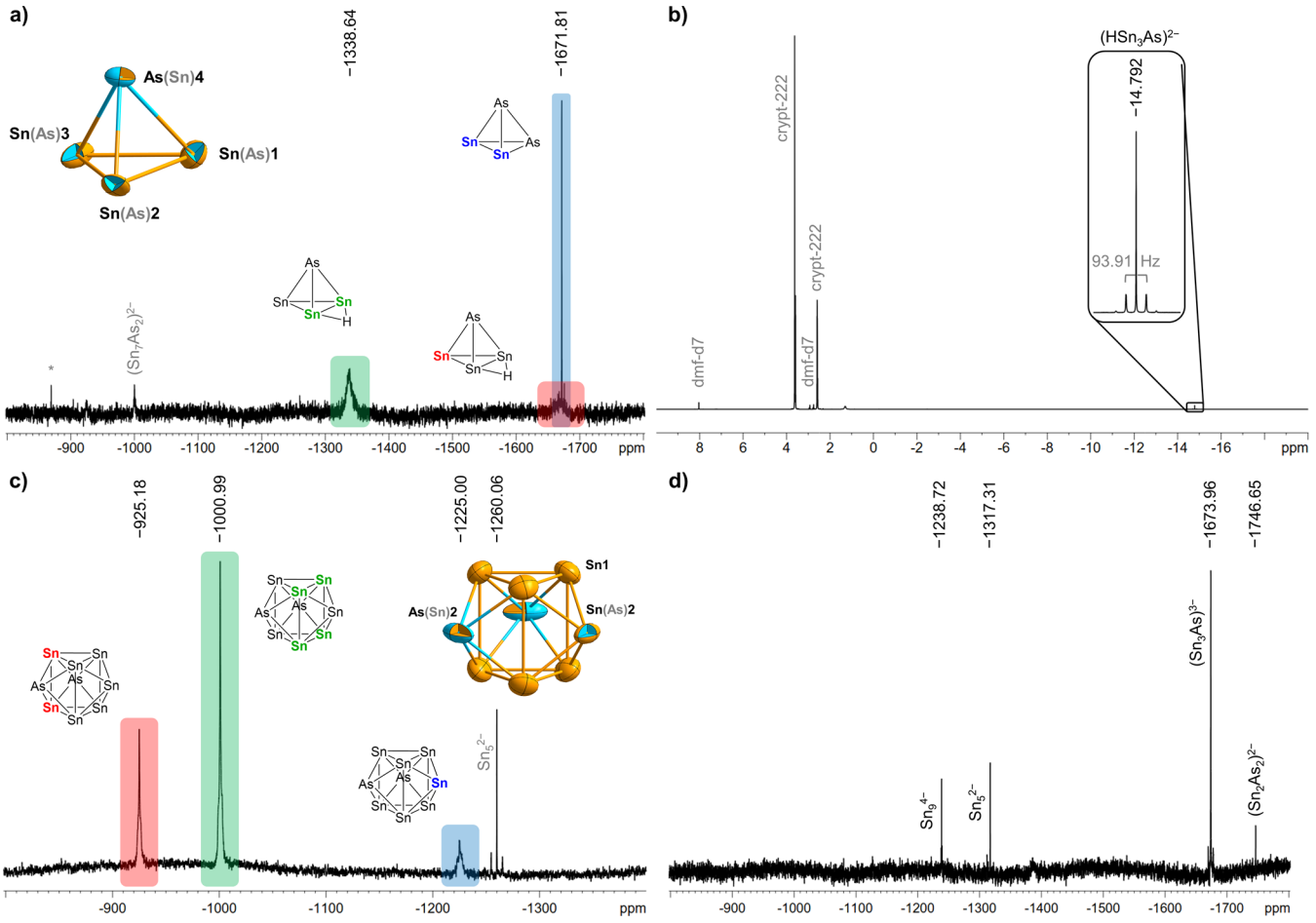


Figure 2. a) Molecular structure of the anion in **2** (thermal ellipsoids drawn at 50% probability, disorder omitted for clarity; the atom type that exhibits the higher site occupancy is emphasized in the two-colored representation of the mixed sites) and ^{119}Sn NMR spectrum (187 MHz) of **2** freshly dissolved in DMF-d_7. Resonances are color-coded to match the corresponding Sn atoms in $(Sn_2As_2)^{2-}$ (blue) and $(HSn_3As)^{2-}$ (green and red). Small amounts of $(Sn_7As_2)^{2-}$ are present alongside an unknown impurity (*) as samples degrade over the duration of the measurement. b) ^{1}H NMR spectrum (500 MHz) of **2** freshly dissolved in DMF-d_7. The inset represents a zoom-in on the resonance of $(HSn_3As)^{2-}$ at high field, exhibiting satellites due to $^1J(^1H,^{119}Sn)$ coupling. c) Molecular structure of the anion in **3** (thermal ellipsoids drawn at 50% probability; of the three symmetry-equivalent atoms bridging the rectangular faces, all of which were refined with a 0.33:0.67 Sn:As occupation, one is highlighted as Sn and two are highlighted as As for illustration) and ^{119}Sn NMR spectrum (187 MHz) of crystals of **3** freshly dissolved in DMF-d_7. Resonances are color-coded to match the corresponding Sn atoms in $(Sn_7As_2)^{2-}$; Sn_5^{2-} is present as a side product. d) ^{119}Sn NMR spectrum (187 MHz) of a freshly filtered solution upon 1 h treatment of 'K_2SnAs' with *en* and crypt-222. As the measurement was conducted in the nondeuterated solvent *en*, a sealed capillary of C_6D_6 was included in the sample.

Table 1. Calculated and Experimental ^{1}H NMR and ^{119}Sn NMR Chemical Shiftsof the Anions in 2 in DMF[a]

Species (Moiety)	Nucleus	$\delta_{calc,DMF}$ [ppm]	$\delta_{exp,DMF}$ [ppm]
$(HSn_3As)^{2-}$	^{1}H	−15.38	−14.79
$(HSn_3As)^{2-}$ (*Sn*−H−*Sn*)	^{119}Sn	−1304	−1339
$(HSn_3As)^{2-}$ (Sn−*Sn*−Sn)	^{119}Sn	−1744	−1670
$(Sn_2As_2)^{2-}$	^{119}Sn	−1773	−1672

[a]Calculated values are obtained at the SO-X2C/TPSSh/x2c-TZVPall-s level, considering 25 DMF molecules explicitly (x2c-SVPall basis for these solvent molecules) and COSMO(DMF) to model long-range interactions with an extended solvent shell.

concentration and the broadness of the resonance renders it not visible, but hidden in the noisy background; a (very) weak signal is detected in the ^{1}H NMR spectrum (Figure S12), suggesting that both species coexist in solution.

Upon addition of a 10-fold excess of toluene to a filtered reaction solution, an orange solid precipitates. The ^{119}Sn NMR spectrum of this solid dissolved in DMF-d_7 shows significant differences. The tentatively assigned resonance disappears, while the resonances for $(Sn_7As_2)^{2-}$ are now present and the resonances for Sn_5^{2-} and $(HSn_3As)^{2-}$ grow considerably. The reason for this observation is unclear; however, we postulate that it relates to the fact that the stability of Zintl anions in the solid state greatly depends on the balance between the sizes of the cation and the anion. Finally, the resonances observed for Sn_5^{2-} in DMF match the theoretical prediction, notably including a resonance shifted highly downfield to +2458 ppm (Figure S13).

In summary, we showed that the treatment of 'K_2SnAs' with *en* is notable for its complexity: Different heteroatomic species can be observed in solution alongside homoatomic species, while the homologous Sn/Bi and Sn/Sb systems selectively yield the respective binary P_4-analogues. The Sn/As system is thus rather comparable to elemental combinations like In/Sb or Tl/Sb, where a large variety of homo- and heteroatomic species crystallize from solution. This increased complexity of

https://doi.org/10.1021/acs.inorgchem.6c04492
Inorg. Chem. XXXX, XXX, XXX−XXX

Downloaded from pubs.acs.org/inocaj/article-pdf/doi/10.1021/acs.inorgchem.6c04492/6918915/acs.inorgchem.6c04492.pdf by KIT BIBLIOTHEK user on 16 November 2026

the process in the solvent may be the result of the relatively larger mismatch of both atomic radii and electron affinities for Sn and As. With the synthesis of the elusive anions $(Sn_2As_2)^{2-}$, $(Sn_7As_2)^{2-}$, and $(HSn_3As)^{2-}$, we also demonstrate the challenges of a sufficiently complete description for the behavior of multinary Zintl solids in solution. Our new addition to the series of binary P_4 analogues is now accessible for use in follow-up reactions with compounds of d- or f-block metals M to form ternary Zintl clusters based on a variety of M/Sn/As elemental combinations.

■ ASSOCIATED CONTENT

Supporting Information

The Supporting Information is available free of charge at https://pubs.acs.org/doi/10.1021/acs.inorgchem.6c04492.

Details on the synthesis, single-crystal X-ray diffraction data, powder X-ray diffraction data, X-ray fluorescence spectroscopy, mass spectrometry data, and quantum chemical studies (PDF)

Archive with all quantum chemical results and optimized structures (ZIP)

Accession Codes

Deposition Numbers 2582091−2582093 contain the supplementary crystallographic data for this paper. These data can be obtained free of charge via the joint Cambridge Crystallographic Data Centre (CCDC) and Fachinformationszentrum Karlsruhe Access Structures service.

■ AUTHOR INFORMATION

Corresponding Authors

Stefanie Dehnen − *Institute of Nanotechnology, Karlsruhe Institute of Technology (KIT), 76131 Karlsruhe, Germany;* orcid.org/0000-0002-1325-9228; Email: stefanie.dehnen@kit.edu

Yannick J. Franzke − *Institute of Nanotechnology, Karlsruhe Institute of Technology (KIT), 76131 Karlsruhe, Germany;* orcid.org/0000-0002-8344-113X; Email: yannick.franzke@kit.edu

Authors

Maximilian Kubis − *Institute of Nanotechnology, Karlsruhe Institute of Technology (KIT), 76131 Karlsruhe, Germany*

Benjamin Peerless − *Institute of Nanotechnology, Karlsruhe Institute of Technology (KIT), 76131 Karlsruhe, Germany*

Complete contact information is available at: https://pubs.acs.org/10.1021/acs.inorgchem.6c04492

Author Contributions

The manuscript was written through contributions of all authors. All authors have given approval to the final version of the manuscript.

Notes

The authors declare no competing financial interest.

■ ACKNOWLEDGMENTS

The authors gratefully acknowledge financial support from the Deutsche Forschungsgemeinschaft (DFG, German Research Foundation) through the Collaborative Research Centre '4f for Future' (CRC 1573, project number 471424360), projects A3 and A4. Y.J.F. gratefully acknowledges financial support via the Walter−Benjamin program funded by the Deutsche Forschungsgemeinschaft (DFG, German Research Foundation)—518707327. This work was partly carried out with the support of the Karlsruhe Nano Micro Facility (KNMFi, www.knmf.kit.edu), an Open Access Research Infrastructure within the Karlsruhe High Technology Hub at the Karlsruhe Institute of Technology (KIT − The University in the Helmholtz Association, www.kit.edu).

■ REFERENCES

(1) Sevov, S. C.; Goicoechea, J. M. Chemistry of Deltahedral Zintl Ions. *Organometallics* **2006**, *25*, 5678−5692.

(2) Scharfe, S.; Kraus, F.; Stegmaier, S.; Schier, A.; Fässler, T. F. Zintl-Ionen, Käfigverbindungen und intermetalloide Cluster der Elemente der 14. und 15. Gruppe. *Angew. Chem.* **2011**, *123*, 3712−3754.

(3) Fässler, T. F. Relationships Between Soluble Zintl Anions, Ligand-Stabilized Cage Compounds, and Intermetalloid Clusters of Tetrel (Si−Pb) and Pentel (P−Bi) Elements. *Struct. Bonding (Berlin)* **2011**, *140*, 91−131.

(4) Wilson, R. J.; Lichtenberger, N.; Weinert, B.; Dehnen, S. Intermetalloid and Heterometallic Clusters Combining p-Block (Semi)Metals with d- or f-Block Metals. *Chem. Rev.* **2019**, *119*, 8506−8554.

(5) Kysliak, O.; Nguyen, D. D.; Clayborne, A. Z.; Schnepf, A. $[PtZn_2Ge_{18}(Hyp)_8]$ (Hyp = $Si(SiMe_3)_3$): A Neutral Polynuclear Chain Compound with $Ge_9(Hyp)_3$ Units. *Inorg. Chem.* **2018**, *57*, 12603−12609.

(6) Zhou, B.; Denning, M. S.; Chapman, T. A. D.; Goicoechea, J. M. Coupling Reactions of Functionalized Zintl Ions $[E_9Cd(C_6H_5)]^{3-}$ (E = Sn, Pb) with Tributyltinhydride: Synthesis and Isolation of $\{Sn_9CdSn[(CH_2)_3CH_3]_3\}^{3-}$. *Inorg. Chem.* **2009**, *48*, 2899−2907.

(7) Lips, F.; Schellenberg, I.; Pöttgen, R.; Dehnen, S. The Subtle Influence of Binary versus Homoatomic Zintl Ions: The Phenyl-Ligated Trimetallic Cage $[Sn_2Sb_5(ZnPh)_2]^{3-}$. *Chem. − Eur. J.* **2009**, *15*, 12968−12973.

(8) Pan, F.; Guggolz, L.; Dehnen, S. Cluster Chemistry with (*Pseudo*-)Tetrahedra Involving Group 13−15 (Semi-)Metal Atoms. *CCS Chem.* **2022**, *4*, 809−824.

(9) Wei, S.; Peerless, B.; Guggolz, L.; Mitzinger, S.; Dehnen, S. Assembly of One to Four As $_4$ Analogues, $(Ge_2As_2)^{2-}$ or $(Ge_3As)^{3-}$, in the Coordination Sphere of $[PhM]^+$, $[MesM]^+$, or M^{2+} (M = Zn, Cd, Hg). *Angew. Chem.* **2023**, *135*, No. e202303037.

(10) Critchlow, S. C.; Corbett, J. D. Heteropolyatomic Anions of the Post Transition Metals. Synthesis and Structure of the Ditindibismuthide(2−) Anion, $Sn_2Bi_2^{2-}$. *Inorg. Chem.* **1982**, *21*, 3286−3290.

(11) Critchlow, S. C.; Corbett, J. D. Heteropolyatomic Anions of the Post Transition Metals. Synthesis and Structure of the Dileaddiantimonide(2-) Anion, $Pb_2Sb_2^{2-}$. *Inorg. Chem.* **1985**, *24*, 979−981.

(12) Xu, L.; Sevov, S. C. Heteroatomic Deltahedral Clusters of Main-Group Elements: Synthesis and Structure of the Zintl Ions $[In_4Bi_5]^{3-}$, $[InBi_3]^{2-}$, and $[GaBi_3]^{2-}$. *Inorg. Chem.* **2000**, *39*, 5383−5389.

(13) Ababei, R.; Heine, J.; Hołyńska, M.; Thiele, G.; Weinert, B.; Xie, X.; Weigend, F.; Dehnen, S. Making Practical Use of the Pseudo-Element Concept: An Efficient Way to Ternary Intermetalloid Clusters by an Isoelectronic Pb−Bi Combination. *Chem. Commun.* **2012**, *48*, 11295.

(14) Lichtenberger, N.; Spang, N.; Eichhöfer, A.; Dehnen, S. Between Localization and Delocalization: $Ru(Cod)^{2+}$ Units in the Zintl Clusters $[Bi_9\{Ru(Cod)\}_2]^{3-}$ and $[Tl_2Bi_6\{Ru(Cod)\}]^{2-}$. *Angew. Chem., Int. Ed.* **2017**, *56*, 13253−13258.

(15) Mitzinger, S.; Bandemehr, J.; Reiter, K.; Scott McIndoe, J.; Xie, X.; Weigend, F.; Corrigan, J. F.; Dehnen, S. $(Ge_2P_2)^{2-}$: A Binary Analogue of P_4 as a Precursor to the Ternary Cluster Anion $[Cd_3(Ge_3P)_3]^{3-}$. *Chem. Commun.* **2018**, *54*, 1421−1424.

(16) Pan, F.; Guggolz, L.; Weigend, F.; Dehnen, S. Atom Exchange Versus Reconstruction: $(Ge_xAs_{4-x})^{x-}$ (x = 2,3) as Building Blocks for

Downloaded from pubs.acs.org/inocaj/article-pdf/doi/10.1021/acs.inorgchem.6c04492/6918961 5/acs.inorgchem.6c04492.pdf by KIT BIBLIOTHEK user on 16 November 2026

the Supertetrahedral Zintl Cluster $[Au_6(Ge_3As)(Ge_2As_2)_3]^{3-}$. *Angew. Chem., Int. Ed.* **2020**, *59*, 16638−16643.
(17) Beuthert, K.; Pan, F.; Guggolz, L.; Wilson, R. J.; Hempelmann, J.; Dronskowski, R.; Dehnen, S. Between Elemental Match and Mismatch: From K_{12} $Ge_{3.5}$ Sb_6 to Salts of $(Ge_2Sb_2)^{2-}$, $(Ge_4Sb_{12})^{4-}$, and $(Ge_4Sb_{14})^{4-}$. *Angew. Chem., Int. Ed.* **2022**, *61*, No. e202207232.
(18) Beuthert, K.; Spang, N.; Alzate Millan, D. C.; Guggolz, L.; Dehnen, S. Expanding the Toolbox: Synthesis of Zintl Salts Containing Anions of the In/Sb and Tl/Sb Elemental Combinations. *Inorg. Chem.* **2025**, *64*, 8711−8718.
(19) Guggolz, L.; Dehnen, S. Systematic DFT Studies on Binary Pseudo-tetrahedral Zintl Anions: Relative Stabilities and Reactivities towards Protons, Trimethylsilyl Groups, and Iron Complex Fragments. *Chem. − Eur. J.* **2020**, *26*, 11819−11828.
(20) Pan, F.; Wei, S.; Guggolz, L.; Eulenstein, A. R.; Tambornino, F.; Dehnen, S. Insights into Formation and Relationship of Multimetallic Clusters: On the Way toward Bi-Rich Nanostructures. *J. Am. Chem. Soc.* **2021**, *143* (18), 7176−7188.
(21) Wilson, R. J.; Dehnen, S. $Ge_4Bi_{14})^{4-}$: A Case of "Element Segregation" on the Molecular Level. *Angew. Chem., Int. Ed.* **2017**, *56*, 3098−3102.
(22) Spang, N.; Beuthert, K.; Kirsch, T. Z.; Guggolz, L.; Franzke, Y. J.; Dehnen, S. From 'KGeP' to the Protonated P_4-like Anion $(HGe_3P)^{2-}$ and the Endohedral Zintl Cluster $[Mn@Ge_{10}P_2]^{3-}$. *J. Am. Chem. Soc.* **2026**, 149.
(23) Knapp, C. M.; Large, J. S.; Rees, N. H.; Goicoechea, J. M. A Versatile Salt-Metathesis Route to Heteroatomic Clusters Derived from Phosphorus and Arsenic Zintl Anions. *Dalton Trans* **2011**, *40*, 735−745.
(24) Pan, F.-X.; Xu, C.-Q.; Li, L.-J.; Min, X.; Wang, J.-Q.; Li, J.; Zhai, H.-J.; Sun, Z.-M. A Niobium-Necked Cluster $[As_3Nb(As_3Sn_3)]^{3-}$ with Aromatic Sn_3^{2-}. *Dalton Trans* **2016**, *45*, 3874−3879.
(25) von Schnering, H.-G.; Wolf, J.; Weber, D.; Ramirez, R.; Meyer, T. $[NbAs_8]^{3-}$, a Novel Type of Complex and an Unexpected One-Dimensional Chain Structure: $_\infty^1[Rb\{NbAs_8\}]^{2-}$. *Angew. Chem., Int. Ed.* **1986**, *25*, 353−354.
(26) Mitzinger, S.; Broeckart, L.; Massa, W.; Weigend, F.; Dehnen, S. $[V@Ge_8As_4]^{3-}$ and $[Nb@Ge_8As_6]^{3-}$: encapsulation of electron-poor transition metal atoms. *Chem. Commun.* **2015**, *51*, 3866.
(27) Edwards, P. A.; Corbett, J. D. Stable Homopolyatomic Anions. Synthesis and Crystal Structures of Salts Containing the Pentaplumbide(2−) and Pentastannide(2−) Anions. *Inorg. Chem.* **1977**, *16*, 903−907.
(28) Wilson, R. J.; Hastreiter, F.; Reiter, K.; Büschelberger, P.; Wolf, R.; Gschwind, R. M.; Weigend, F.; Dehnen, S. $[Co@Sn_6Sb_6]^{3-}$: An Off-Center Endohedral 12-Vertex Cluster. *Angew. Chem., Int. Ed.* **2018**, *57*, 15359−15363.
(29) Wilson, W. L.; Rudolph, R. W.; Lohr, L. L.; Taylor, R. C.; Pyykkö, P. *Inorg. Chem.* **1986**, *25*, 1535−1541.
(30) Peng, D.; Middendorf, N.; Weigend, F.; Reiher, M. An efficient implementation of two component relativistic exact decoupling methods for large molecules. *J. Chem. Phys.* **2013**, *138*, 184105.
(31) Franzke, Y. J.; Middendorf, N.; Weigend, F. Efficient implementation of one- and two-component analytical energy gradients in exact two-component theory. *J. Chem. Phys.* **2018**, *148*, 104110.
(32) Franzke, Y. J. Reducing exact two-component theory for NMR couplings to a one-component approach: efficiency and accuracy. *J. Chem. Theory Comput.* **2023**, *19*, 2010−2028.
(33) Franzke, Y. J.; Weigend, F. NMR shielding tensors and chemical shifts in scalar-relativistic local exact two-component theory. *J. Chem. Theory Comput.* **2019**, *15*, 1028−1045.
(34) Franzke, Y. J.; Mack, F.; Weigend, F. NMR indirect spin−spin coupling constants in a modern quasi-relativistic density functional framework. *J. Chem. Theory Comput.* **2021**, *17*, 3974−3994.
(35) Franzke, Y. J.; Holzer, C. Exact two-component theory becoming an efficient tool for NMR shieldings and shifts with spin−orbit coupling. *J. Chem. Phys.* **2023**, *159*, 184102.
(36) Staroverov, V. N.; Scuseria, G. E.; Tao, J.; Perdew, J. P. Comparative assessment of a new nonempirical density functional: Molecules and hydrogen-bonded complexes. *J. Chem. Phys.* **2003**, *119*, 12129−12137.
(37) Franzke, Y. J.; Treß, R.; Pazdera, T. M.; Weigend, F. Error consistent segmented contracted all electron relativistic basis sets of double and triple-ζ quality for NMR shielding constants. *Phys. Chem. Chem. Phys.* **2019**, *21*, 16658−16664.
(38) Rudolph, R. W.; Wilson, W. L.; Parker, F.; Taylor, R. C.; Young, D. C. Nature of Naked-Metal-Cluster Polyanions in Solution. Evidence for $(Sn_{9-x}Pb_x)^{4-}$(x = 0−9) and Tin-Antimony Clusters. *J. Am. Chem. Soc.* **1978**, *100*, 4629−4630.

Downloaded from pubs.acs.org/inocaj/article-pdf/doi/10.1021/acs.inorgchem.6c04492/6918961 5/acs.inorgchem.6c04492.pdf by KIT BIBLIOTHEK user on 16 November 2026

https://doi.org/10.1021/acs.inorgchem.6c04492
Inorg. Chem. XXXX, XXX, XXX−XXX